

Analytic model of near-field radio-frequency sheaths:

I. Tenuous plasma limit

D. A. D'Ippolito and J. R. Myra

*Lodestar Research Corporation,
Boulder, Colorado, 80301*

August, 2008

Submitted to Phys. Plasmas

DOE/ER/54392-49

LRC-08-125

Lodestar Research Corporation

2400 Central Avenue #P-5

Boulder, CO 80301

Analytic model of near-field radio-frequency sheaths:

I. Tenuous plasma limit

D. A. D’Ippolito[†] and J. R. Myra

Lodestar Research Corporation, 2400 Central Avenue, Boulder, Colorado 80301

Abstract

An analytic model is derived for electromagnetic radio-frequency (rf) wave propagation in a waveguide filled by a tenuous plasma with a slightly tilted equilibrium magnetic field \mathbf{B} , i.e. $b_y = B_y / B \ll 1$. The calculation includes the self-consistent coupling between the rf fields and the sheaths at the sheath-plasma interface, and can be used to describe antenna sheath formation in the ion cyclotron range of frequencies (ICRF). The sheaths are treated as thin vacuum regions separating the plasma and metal wall. It is shown that (i) the launched fast wave is coupled parasitically to the slow wave by the magnetic field structure when $b_y \neq 0$ and by the sheath BC; (ii) the sheath voltage V_{sh} is dependent on the wave parity (the “antenna phasing”); and (iii) integrating the vacuum rf fields, $V_{vac} = -\int dz E_{\parallel}^{(vac)}$, gives an overestimate of the sheath voltage. An expression for the self-consistent V_{sh} including plasma effects and satisfying the Child-Langmuir Law is obtained.

PACS numbers: 52.35.Mw, 52.40.Kh, 52.50.Qt, 52.55.Fa

[†]email: dippolito@lodestar.com

Introduction

Radiofrequency (rf) waves in the ion cyclotron range of frequencies (ICRF) have been used to heat and drive current successfully in many fusion experiments. In designing and operating such an rf system, one of the important areas of optimization is to reduce deleterious antenna-edge plasma interactions. Launching megawatts of fast wave (FW) power into the scrape-off-layer (SOL) plasma can lead to strongly nonlinear interactions associated with the unwanted but parasitically-coupled slow wave (SW). A review of the early history of observed antenna-plasma interactions in experiments is given in Ref. 1 and a review of important nonlinear mechanisms is given in Ref. 2. About twenty years ago, it was realized that one of the most important interactions with high-power ICRF antennas in tokamaks is the formation of high-voltage rf sheaths induced by the parasitic SW.³⁻⁷ The SW polarization has a substantial rf electric field component (E_{\parallel}) parallel to \mathbf{B} ; the E_{\parallel} component accelerates electron losses along open field lines into nearby boundaries, and a large sheath potential forms to restore ambipolarity by confining electrons. The dc sheath potential accelerates ions out of the plasma, causing material damage to the walls by sputtering and local heating, and also resulting in a parasitic power loss (often referred to as “sheath power dissipation”).²

The generation of the parasitic SW occurs when the local magnetic field line does not have perfect alignment, i.e. it is not orthogonal to the current straps of the antenna and/or not parallel to the conducting boundaries (antenna, limiters and wall). The former effect drives the SW electric field directly, and the latter effect requires the coupling of SW to FW to allow the rf electric field boundary conditions^{8,9} (BC) to be satisfied. The strength of the SW and the resulting sheath potential depends on the antenna phasing, the magnetic geometry, the local plasma density, and other parameters.

Early explorations of sheath formation on antennas^{7,10} (and subsequent studies) used a “vacuum rf field sheath approximation”, in which the oscillating (ac) sheath

voltage V was estimated by integrating the E_{\parallel} component of the vacuum rf electric field along each field line between contact points, i.e. $V = \oint ds E_{\parallel}$. This approach has been very useful in developing a *qualitative* understanding, and it has been implemented as a diagnostic in several 3D antenna codes.¹⁰⁻¹² However, *quantitative* results require that the rf field calculation take into account the presence of plasma and ensure that the rf field satisfies a sheath BC at the conducting surfaces. In the simplest model,⁹ the sheath is treated as a thin vacuum region separating the plasma from the conducting wall, and the continuity of the normal component of $\mathbf{D} = \epsilon \cdot \mathbf{E}$ is enforced. Similar BCs have been used in plasma processing (for example, see Refs. 13 and 14). The effect of this BC results in a certain amount of screening of the E_{\parallel} component from the high-dielectric plasma region, so that the rf field structure is modified by the presence of the sheaths. The sheath BC can be applied for an assumed sheath width Δ , but a self-consistent solution requires nonlinear rootfinding or iteration to ensure that Δ satisfies the Child-Langmuir Law at all points on the boundary. This is a difficult computational problem for a 3D antenna or wave propagation code.

The goal of the present paper is to illustrate the effect of the sheath BC on electromagnetic wave (coupled FW-SW) propagation in a plasma channel with metal boundaries. We view this plasma-filled waveguide approach as a simplified description (without unnecessary geometric complications) of the wave propagation in the front of an ICRF antenna and will refer to it generically as an “antenna model”. The calculation illustrates analytically many of the key features that were explored numerically in previous studies of antenna sheaths. The most important application of this model is to evaluate the corrections to the vacuum rf field approximation in evaluating antenna sheath voltages.

The plan of this paper is as follows. In Sec. II, the model is described, the wave propagation equations are solved using a perturbation expansion in the small poloidal

magnetic field, $b_y \equiv B_y/B \ll 1$, and a low-density (“tenuous plasma”) approximation described subsequently. The sheath BC is applied to obtain a solution of the bounded problem for fixed sheath width Δ . It is shown that the magnetic field tilt b_y and the sheath BC couples the propagating FW to a driven SW. In Sec. III, the physical consequences of the parasitic SW are examined. First, the sheath voltage V_{sh} and the voltage split between the plasma and sheath regions are calculated and plasma screening of E_{\parallel} is demonstrated. Second, the Child-Langmuir constraint is applied and the self-consistent wave and sheath parameters (E_{\parallel} , Δ , V_{sh}) are calculated. In Sec. IV the model is applied to compute the phasing dependence of the antenna sheath potential and to obtain plasma corrections to the vacuum rf field model. A summary of the work and conclusions are given in Sec. V.

I. RF field solution

Consider the problem of electromagnetic wave (coupled FW and SW) propagation down a waveguide filled by a constant-density plasma which is tenuous enough that we can set $\epsilon_x = 0$ and $\epsilon_{\perp} = 1$ but keep $|\epsilon_{\parallel}| \gg 1$. The FW is assumed to be polarized in the y direction; it is launched at $x = 0$ and propagates in the +x direction. The equilibrium magnetic field is given by $\mathbf{B} = B(\hat{e}_z + b_y \hat{e}_y)$ with $b_y \equiv B_y/B \ll 1$, and the magnetic field lines intersect conducting walls at $z = \pm L$. To simplify the expressions even further, we set $k_y = 0$. Thus, the field line tilt is assumed to be small, and we solve the wave propagation problem using a perturbation expansion in the small parameter b_y . In making the correspondence with an antenna in a tokamak, (x, y, z) correspond to the radial, poloidal, and toroidal directions, respectively.

This model problem is meant to approximate the fields near the front face of a FW antenna where the density is low, the FW field is polarized in the direction of the (poloidal) current straps, and the equilibrium magnetic field typically has a small component in the direction of the current straps. The situation where the magnetic field is

perfectly aligned with respect to the antenna ($\mathbf{B} \cdot \mathbf{J}_a = 0$) almost never occurs in practice, but the misalignment is often small, justifying the perturbation expansion used here. The boundaries at $z = \pm L$ represent the antenna frame or antenna protection limiters that enclose a typical FW antenna.

A. Basic equations

The wave equation is $\mathbf{L}\mathbf{E} = -(4\pi i/\omega)\mathbf{J}_a$, where the wave propagation operator is

$$\mathbf{L} = -\frac{c^2}{\omega^2} \nabla \times (\nabla \times \mathbf{E}) + \boldsymbol{\varepsilon} \cdot \mathbf{E} = \mathbf{n} \times (\mathbf{n} \times \mathbf{E}) + \boldsymbol{\varepsilon} \cdot \mathbf{E} = (\mathbf{n}\mathbf{n} - n^2\mathbf{I} + \boldsymbol{\varepsilon}) \cdot \mathbf{E} . \quad (1)$$

Here, \mathbf{E} is the rf electric field, \mathbf{J}_a is the antenna current density, $\mathbf{n} = \mathbf{k}c/\omega$ is the the index of refraction, \mathbf{k} is the wavenumber, ω is the rf frequency, \mathbf{I} is the unit tensor and $\boldsymbol{\varepsilon} = \varepsilon_{\perp}\mathbf{I} + (\varepsilon_{\parallel} - \varepsilon_{\perp})\mathbf{b}\mathbf{b} + (i\varepsilon_{\times}/2)(\mathbf{b} \times \mathbf{I} + \mathbf{I} \times \mathbf{b})$ is the plasma dielectric tensor. A treatment of the wave propagation problem using the full plasma dielectric tensor $\boldsymbol{\varepsilon}$ will be given in a later paper. In the present paper, we illustrate the physics in its simplest form by making use of the ‘‘tenuous plasma approximation’’ for the plasma dielectric tensor $\boldsymbol{\varepsilon}$, viz.

$$\varepsilon_{\perp} = 1 - \frac{\omega_{pi}^2}{(\omega^2 - \Omega_i^2)} \rightarrow 1 , \quad \varepsilon_{\times} = \frac{\omega_{pi}^2 \omega}{\Omega_i(\omega^2 - \Omega_i^2)} \rightarrow 0 , \quad \varepsilon_{\parallel} = 1 - \frac{\omega_{pe}^2}{\omega^2} . \quad (2)$$

so that $\boldsymbol{\varepsilon} = \mathbf{I} + (\varepsilon_{\parallel} - 1)\mathbf{b}\mathbf{b}$. This approximation is valid when $\omega > \Omega_i$ and $\omega_{pi}^2 \ll \omega^2 \ll \omega_{pe}^2$. Expanding in powers of b_y , the plasma dielectric tensor to first order has the form $\boldsymbol{\varepsilon} = \boldsymbol{\varepsilon}_0 + \boldsymbol{\varepsilon}_1$, where $\boldsymbol{\varepsilon}_0 = \mathbf{I} + (\varepsilon_{\parallel} - 1)\mathbf{e}_z\mathbf{e}_z$ and $\boldsymbol{\varepsilon}_1 = (\varepsilon_{\parallel} - 1)(\mathbf{b}_y\mathbf{e}_z + \mathbf{e}_z\mathbf{b}_y)$.

For a homogeneous plasma the undriven problem, $\mathbf{L}\mathbf{E} = 0$, yields the following dispersion relations for the FW (subscript f) and SW (subscript s) in the tenuous plasma model:

$$n_f^2 = 1 \quad (3)$$

$$n_{xs}^2 + \varepsilon_{\parallel}(n_{zs}^2 - 1) = 0 \quad (4)$$

where $n_f^2 \equiv n_{xf}^2 + n_{zf}^2$. To complete the specification of the problem, the following BCs⁹ are imposed at the sheath-plasma interface at $z = +L$ (for solutions with definite parity the BC at $z = -L$ is redundant.):

$$E_x = -\Delta\epsilon_{\parallel} \frac{\partial E_z}{\partial x}, \quad E_y = -\Delta\epsilon_{\parallel} \frac{\partial E_z}{\partial y} \rightarrow 0 \quad (5)$$

where $k_y = 0$ was used in the last step. This BC is equivalent to enforcing continuity of the normal component of \mathbf{D} (here, $D_z \equiv \epsilon_{zz}E_z \approx \epsilon_{\parallel}E_z$) across the sheath-plasma interface. The term on the rhs of the BC describes the effect on the rf fields of the sheath capacitance, where Δ is the sheath width in z . In the limit $\Delta \rightarrow 0$, we recover the usual “metal wall” BC, viz. that the tangential component of \mathbf{E} vanishes. Here, “normal” and “tangential” are defined with respect to the sheath / wall.

B. FW solution

In lowest order, the wave equation is

$$L_0\mathbf{E}_0 = -(4\pi i / \omega) J_a \mathbf{e}_y, \quad (6)$$

where J_a is the FW antenna current at $x = 0$. Instead of specifying the current, we can set $J_a = 0$ and equivalently specify the fast wave amplitude E_{0y} at $x = 0$. The lowest order equation becomes

$$L_0\mathbf{E}_0 = \begin{pmatrix} 1-n_z^2 & 0 & n_x n_z \\ 0 & 1-n^2 & 0 \\ n_x n_z & 0 & \epsilon_{\parallel} - n_x^2 \end{pmatrix} \begin{pmatrix} E_x \\ E_y \\ E_z \end{pmatrix} = 0. \quad (7)$$

and the y component equation gives the following solution for the FW polarization

$$\mathbf{E}_0 = \mathbf{E}_f = \{0, \hat{E}_y \cos(k_{zf}z - \delta), 0\} e^{ik_{xf}x}, \quad (8)$$

where \hat{E}_y is the maximum amplitude of the FW, and we use the vector notation $\mathbf{E} = \{E_x, E_y, E_z\}$. Two definite-parity cases are considered for the phase δ in Eq. (8):

$\delta = 0$, which models *monopole* phasing of a two-strap antenna (E_y has even parity in z); and $\delta = \pi/2$, corresponding to *dipole* phasing (E_y has odd parity in z). Here, k_{zf} is determined by the BC on E_y at the sheath, and k_{xf} is given by the FW dispersion relation, Eq. (3). Applying the E_y BC in Eq. (5) to the FW, we obtain the constraint $\cos(k_{zf}L - \delta) = 0$, requiring that $\eta_{zf} \equiv k_{zf}L = \pi/2 + \delta$. For future use, we also define a normalized vacuum wavenumber, $\eta_0 \equiv \omega L/c$, which satisfies the identity

$$\eta_0 n_{zf} = \eta_{zf} \equiv (\pi/2)\alpha \quad (9)$$

where $\alpha = 1 + (2\delta/\pi)$ to satisfy the FW BC.

To first order in b_y , the wave equation becomes $L_0 \mathbf{E}_1 = -\epsilon_1 \mathbf{E}_0$, or explicitly

$$\begin{pmatrix} 1-n_z^2 & 0 & n_x n_z \\ 0 & 1-n^2 & 0 \\ n_x n_z & 0 & \epsilon_{\parallel} - n_x^2 \end{pmatrix} \begin{pmatrix} E_{1x} \\ E_{1y} \\ E_{1z} \end{pmatrix} = - \begin{pmatrix} 0 & 0 & 0 \\ 0 & 0 & b_y(\epsilon_{\parallel} - 1) \\ 0 & b_y(\epsilon_{\parallel} - 1) & 0 \end{pmatrix} \begin{pmatrix} 0 \\ \hat{E}_y \\ 0 \end{pmatrix} \cos(k_{zf}z - \delta) e^{ik_{xf}x}. \quad (10)$$

In general, we have $\mathbf{E}_1 = \mathbf{E}_{1p} + \mathbf{E}_{1h}$, where the subscripts p and h denote the ‘‘particular’’ and ‘‘homogeneous’’ solutions of Eq. (10). We see that \mathbf{E}_{1p} is driven by the FW rf electric field when E_y has a component along \mathbf{B} ($b_y \neq 0$). In general, \mathbf{E}_{1h} is also needed to satisfy the full BC.

In carrying out the waveguide solution (having finite extent in z , not a plane wave), the index of refraction \mathbf{n} is treated as an operator, $\mathbf{n} \rightarrow -i(c/\omega)\nabla$. The x -component of Eq. (10) requires that the solution have the SW polarization. The z -component of Eq. (10) is driven by the FW and therefore requires that the solution have $k_x = k_{xf}$ and $k_z = k_{zf}$. To satisfy these conditions, we employ the ansatz $E_{1z} = C \cos(k_{zf}z - \delta) e^{ik_{xf}x}$. Combining these equations and using the FW dispersion

relation, Eq. (3), to simplify the resulting expression for C , we obtain the particular solution

$$\mathbf{E}_{1p} = C \{iG_f \sin(k_{zf}z - \delta), 0, \cos(k_{zf}z - \delta)\} e^{ik_{xf}x}, \quad (11)$$

where $C = -b_y \hat{E}_y$ and $G_j \equiv n_{xj} n_{zj} / (n_{zj}^2 - 1)$ for $j = f$ or s . The quantities $n_{xj} = k_{xj} c / \omega$ and $n_{zj} = k_{zj} c / \omega$ in G_j are defined to be scalars (not operators). Note that $\mathbf{b} \cdot \mathbf{E}_f = b_y \hat{E}_y$, so that C is proportional to the part of E_{\parallel} driven directly by the FW and thus provides the electron acceleration necessary for sheath formation.

C. SW solution

It is easy to show that the superposition $\mathbf{E}_0 + \mathbf{E}_{1p}$ does not satisfy the sheath BC for E_x in Eq. (5). To satisfy this BC, the FW must couple to another wave which has the SW polarization (with $E_x \neq 0$) and satisfies the SW dispersion relation ($k_x = k_{xs}$, $k_z = k_{zs}$). The desired SW is given by the x - and z -components of the homogeneous equations, Eq. (7); thus, it has the same polarization as the solution in Eq. (11) but with a different amplitude and SW wavenumbers:

$$\mathbf{E}_{1h} = \mathbf{E}_s = A \{iG_s \sin(k_{zs}z - \delta), 0, \cos(k_{zs}z - \delta)\} e^{ik_{xs}x}. \quad (12)$$

The coefficient A is determined by applying the x -component of the sheath BC in Eq. (5) at the sheath-plasma interface ($z = L$):

$$\left(E_x + \Delta \epsilon_{\parallel} \frac{\partial E_z}{\partial x} \right)_{z=L} = i(CD_f e^{ik_{xf}x} + AD_s e^{ik_{xs}x}) = 0. \quad (13)$$

Here, we define $D_j = D(\eta_{zj})$ and $\eta_{zj} \equiv k_{zj}L$ with $j = f, s$. The function $D(\eta)$ is a global dispersion function for the coupled sheath-plasma system given by

$$D(\eta_{zj}) \equiv G_j \sin(\eta_{zj} - \delta) + k_{xj} \Delta \epsilon_{\parallel} \cos(\eta_{zj} - \delta). \quad (14)$$

This function involves the homogeneous FW and SW dispersion relations (through k_x and k_z), the plasma density (through $\epsilon_{||}$), the system length L (in η), the sheath width Δ , and the wave phase. The first term in D represents the usual metal wall BC ($E_{\tan} = 0$) whereas the second term contains the sheath capacitance effect.

We see that the solution of Eq. (13) requires two conditions. First, we must require

$$k_{xs} = k_{xf} \equiv k_x \quad (15)$$

to obtain a solution that is valid for all x . Then we can solve for the value of the SW amplitude A that solves the BC, viz.

$$A = -C \frac{D_f}{D_s} = b_y \hat{E}_y \frac{G_f}{D_s} . \quad (16)$$

In the last step, we used the result for C obtained in Eq. (11) and the relation $\eta_{zf} - \delta = \pi/2$, obtained from applying the BC on E_y to the FW. Using the latter result, we find that the second term in D_f vanishes and $D_f = G_f$ for any value of δ .

To summarize, the sum of the three waves $\mathbf{E}_0 + \mathbf{E}_{1p} + \mathbf{E}_{1h}$ satisfies the full sheath BC when the SW amplitude A satisfies Eq. (16). In terms of our ordering, $A \propto b_y E_{0y}$ is a first order quantity, so the total first order response to the FW is $\mathbf{E}_1 = \mathbf{E}_{1p} + \mathbf{E}_{1h}$, given by

$$\begin{aligned} E_{1x} &= -i b_y \hat{E}_y \left(G_f \sin(k_{zf}z - \delta) - \frac{G_f}{D_s} G_s \sin(k_{zs}z - \delta) \right) e^{ik_x x} , \\ E_{1y} &= 0 , \\ E_{1z} &= -b_y \hat{E}_y \left(\cos(k_{zf}z - \delta) - \frac{G_f}{D_s} \cos(k_{zs}z - \delta) \right) e^{ik_x x} . \end{aligned} \quad (17)$$

Here, the quantity D_s is defined by Eq. (14) and the wave polarization coefficients $G_j \equiv n_{xj} n_{zj} / (n_{zj}^2 - 1)$ can be simplified as follows. The FW dispersion relation gives

$G_f = -n_{zf} / n_{xf}$. To evaluate G_s , we rewrite the SW dispersion relation (4) in the form $n_{zs}^2 - 1 = -n_x^2 / \epsilon_{\parallel}$, implying that $n_{zs}^2 \approx 1$ when $\epsilon_{\parallel} \gg n_x^2$. It follows that $G_s \approx -\epsilon_{\parallel} / n_{xs} \approx -\epsilon_{\parallel} / (n_{xs} n_{zs})$. Thus, we have derived the following forms for the functions D_j and G_j

$$\begin{aligned} D_f &= G_f = -n_{zf} / n_x, & G_s &= -\epsilon_{\parallel} / (n_{xs} n_{zs}) \approx -\epsilon_{\parallel} / n_x, \\ D_s &\equiv G_s \sin(\eta_{zs} - \delta) + k_x \Delta \epsilon_{\parallel} \cos(\eta_{zs} - \delta). \end{aligned} \quad (18)$$

The physical interpretation of Eq. (17) is as follows. The electric field terms with $k_z = k_{zf}$ describe the wave generated by the misalignment of the magnetic field ($b_y \neq 0$) with respect to the FW polarization. The terms in \mathbf{E}_1 with $k_z = k_{zs}$ describe the SW generated at the sheath-plasma interface in order to satisfy the sheath BC. So the first order response to the driving FW comes about from two effects.

Note that the SW terms in Eq. (17) are proportional to $1/D_s$, implying the possibility of a resonance when the two terms in D_s nearly cancel [see Eq. (14)]. We refer to this well-known effect¹⁵⁻¹⁹ as the “sheath-plasma wave resonance.” The first term in D_s (shown above to be proportional to ϵ_{\parallel}) is related to the inductive plasma current into the sheath, and the second term (proportional to Δ) is related to the capacitive current across the sheath. In some cases the system (plasma + sheath) can form a resonant LC circuit, leading to large electric fields and sheath potentials. Examples include plasma processing applications¹⁸ and “far field” sheaths in tokamaks.¹⁹ In the present problem, we do not expect the sheath plasma resonance to be accessible because k_x (in the second term of D_s) does not satisfy the usual SW ordering; it is constrained to equal the much smaller FW value. It will be shown subsequently that in the present problem the denominator can be written in a positive definite form for most cases of interest.

II. Slow wave effects

A. Sheath voltage

An important application of this model is to calculate the sheath voltage V_{sh} taking into account the self-consistent response of the rf fields to the presence of the sheath capacitance.

The ac sheath voltage V_{sh} across one sheath (e.g. at $z = L$) is given by

$$V_{\text{sh}} \equiv - \int_{\text{sh}} dz E_z^{(\text{sh})} = -\Delta \left(\epsilon_{zz}^{(0)} E_{1z}(L) + \epsilon_{zy}^{(1)} E_{0y}(L) \right) = -\Delta \epsilon_{\parallel} E_z(L) , \quad (19)$$

where the superscripts on ϵ denote the order of the dielectric tensor element in powers of b_y . In the second equality, the continuity of the component of \mathbf{D} normal to the sheath ($D_n = -\hat{e}_z \cdot \mathbf{D} = \text{const.}$) is used to relate $E_z^{(\text{sh})}$ to E_z on the plasma side of the sheath-plasma interface, treating the sheath as a vacuum layer ($\epsilon_{\text{sh}} = 1$). In the last relation, we use the constraint in Eq. (5) that $E_{0y}(L) = 0$ to satisfy the FW BC. The phase of this oscillating rf sheath voltage is arbitrary, so the overall sign was chosen for convenience in defining the following dimensionless voltage:

$$\hat{V} \equiv \frac{-\pi V_{\text{sh}} e^{-ik_x x}}{2 b_y \hat{E}_y L} = \frac{\pi \Delta \epsilon_{\parallel}}{2 L} \frac{D_f}{D_s} \cos(\eta_{zs} - \delta) \quad (20)$$

derived from Eqs. (17) and (19). Using the definitions in Eq. (18) and after doing a short calculation, this result can be put in the simple form

$$\hat{V} = \frac{(\Delta/L) n_{zf}^2 \eta_0 \cos(\eta_0 - \delta)}{(\Delta/L)(n_{zf}^2 - 1) \alpha \eta_0 \cos(\eta_0 - \delta) + \alpha \sin(\eta_0 - \delta)} . \quad (21)$$

This calculation also required the following identities: $n_{zs} \approx 1$ (SW dispersion relation with $\epsilon_{\parallel} \gg n_x^2$), $\eta_{zs} = \eta_0 n_{zs} \approx \eta_0$ where $\eta_0 \equiv \omega L / c$, and $\eta_0 n_{zf} \equiv \eta_{zf} = \alpha \pi / 2$ [see Eq. (9)]. Here, $\alpha \equiv 1 + (2\delta / \pi) = 1$ for monopole and $\alpha = 2$ for dipole.

Note that \hat{V} is *symmetric* with respect to η in monopole phasing ($\delta = 0$) but *anti-symmetric* in dipole phasing ($\delta = \pi/2$). Thus, the model possesses the correct symmetry to give magnetic flux addition / cancellation⁷ when the effect of the sheath voltages at $z = \pm L$ are combined to calculate the time-averaged (rectified) sheath potential (this combination is valid when the sheaths are correlated, e.g. in the mobile electron limit, $v_{\parallel} / \omega L > 1$).

The ratio \hat{V} can be given a physical interpretation in terms of the sheath voltage V_{vac} in the “vacuum field sheath model.” The latter voltage is computed by integrating the rf E_{\parallel} component along the field line between sheaths,³⁻⁷ $V_{\text{vac}} = -\int dz E_{\parallel}^{(\text{vac})}$. In the present model, for monopole phasing ($\delta = 0$), the vacuum approximation to the voltage across one sheath is

$$V_{\text{vac}}(\delta = 0) = -\int_0^L dz b_y \hat{E}_y \cos k_{zf} z e^{ik_x x} = -\frac{2}{\pi} b_y E_{y0} L e^{ik_x x} . \quad (22)$$

This quantity takes into account only the lowest order FW field, neglecting the plasma response to the BC. The first equality in Eq. (20) can be rewritten as

$$\hat{V}(\delta) \equiv V_{\text{sh}}(\delta) / V_{\text{vac}}(0) , \quad (23)$$

showing that $\hat{V}(\delta)$ is the ratio of the sheath voltage for phase δ , including the contributions of both FW and SW fields, normalized to the vacuum sheath voltage in monopole phasing.

The model can be characterized by two dimensionless parameters, e.g. n_{zf} and Δ/L . We are primarily interested in the range corresponding to “short” antennas:

$$1 \leq n_{zf} < \infty \Leftrightarrow \pi/2 \geq \eta_0 > 0 \quad (24)$$

where the FW is radially evanescent in a tenuous plasma. In this range the denominator of \hat{V} does not vanish ($D_s \neq 0$) and there is no sheath-plasma resonance.

Now, consider some limiting cases of Eq. (21). For monopole phasing, in the limit $n_{zf} \gg 1$ (which implies $\eta_0 \ll 1$), we find

$$\hat{V}(0) = \frac{(\Delta/L)n_{zf}^2}{1 + (\Delta/L)n_{zf}^2} \equiv \mathfrak{R} . \quad (25)$$

Taking sub-limits of \mathfrak{R} , this expression reduces to

$$\hat{V}(0) = 1 , \quad \text{for } (\Delta/L)n_{zf}^2 \gg 1 , \quad (26)$$

$$\hat{V}(0) = (\Delta/L)n_{zf}^2 \ll 1 , \quad \text{for } (\Delta/L)n_{zf}^2 \ll 1 . \quad (27)$$

This is one of our main results and shows that the ‘‘vacuum field sheath model’’ gives the correct result in the limit of large $(\Delta/L)n_{zf}^2$ but overestimates the sheath voltage in the opposite limit.

Another interesting case is $n_{zf} \sim 1$ (and hence $\eta_0 \sim 1$) but $\Delta/L \ll 1$. For any phasing, Eq. (21) reduces to

$$\hat{V} = (\Delta/L)n_{zf}^2 \eta_0 \cot(\eta_0 - \delta) / \alpha \ll 1 \quad (28)$$

B. Plasma E_{\parallel}

Another interesting consequence of the sheath BC is illustrated in this section, viz. the screening of E_{\parallel} in the plasma and its concentration in the rf sheaths. The rf electric field component in the plasma, which is parallel to the equilibrium field \mathbf{B} , is specified to first order in b_y as

$$\begin{aligned} E_{\parallel} &= E_z + b_y E_y \\ &= [C \cos(k_{zf}z - \delta) + A \cos(k_{zs}z - \delta) + b_y \hat{E}_y \cos(k_{zf}z - \delta)] e^{ik_x x} \end{aligned} \quad (29)$$

where $C = -b_y \hat{E}_y$ and A is given by Eq. (16). Substituting in for C and A , *the first and third terms cancel* leaving

$$E_{\parallel} = b_y \hat{E}_y \frac{D_f}{D_s} \cos(k_{zs}z - \delta) e^{ik_x x} , \quad (30)$$

showing that only the true SW (having both SW polarization and satisfying the SW dispersion relation) contributes to the E_{\parallel} . Using the same manipulations as in Sec. II A, it is straightforward to show that E_{\parallel} in the plasma region is given by

$$E_{\parallel} = \frac{-V_{\text{vac}}(0)}{\alpha \epsilon_{\parallel} L} \left(\frac{n_{zf}^2 \eta_0 \cos(k_{zs}z - \delta)}{\sin(\eta_0 - \delta) + (\Delta/L)(n_{zf}^2 - 1)\eta_0 \cos(\eta_0 - \delta)} \right) , \quad (31)$$

where $V_{\text{vac}}(0)$ is the vacuum voltage defined in Eq. (22). The cancellation just mentioned and the appearance here of $1/\epsilon_{\parallel}$ is the *plasma screening effect*.

The plasma screening effect can be represented by a sheath capacitance parameter Λ defined by⁹

$$\Lambda \equiv -\frac{\epsilon_{\parallel} \Delta}{\epsilon_{\text{sh}} L} , \quad (32)$$

where $\epsilon_{\text{sh}} = 1$ is the scalar dielectric of the (vacuum) sheath region. The parameter Λ characterizes the ratio of the capacitive sheath impedance to the inductive plasma impedance; when $\Lambda = 1$ the two impedances are equal.

Using this definition, E_{\parallel} in Eq. (31) can be rewritten as

$$E_{\parallel} = \frac{V_{\text{vac}}(0)}{\Lambda \alpha L} \left(\frac{(\Delta/L)n_{zf}^2 \eta_0 \cos(k_{zs}z - \delta)}{\sin(\eta_0 - \delta) + (\Delta/L)(n_{zf}^2 - 1)\eta_0 \cos(\eta_0 - \delta)} \right) . \quad (33)$$

To illustrate the effect of screening, we consider the case of monopole phasing ($\delta = 0$ and $\alpha = 1$). Again taking the sub-limit $n_{zf} \gg 1$ (implying that $\eta_0 \ll 1$), Eq. (33) reduces to

$$E_{\parallel}(0) = \frac{V_{\text{vac}}(0)}{L} \frac{\Re}{\Lambda} \cos k_{zs}z , \quad \Re = \frac{(\Delta/L)n_{zf}^2}{1 + (\Delta/L)n_{zf}^2} . \quad (34)$$

Note that $\mathfrak{R} \rightarrow 1$ for $1 \ll L/\Delta \ll n_{zf}^2$ and $\mathfrak{R} \rightarrow 0$ for $1 \ll n_{zf}^2 \ll L/\Delta$. Since \mathfrak{R} is bounded ($0 \leq \mathfrak{R} \leq 1$), the main result here is that the parallel component of the SW is completely screened from the plasma in the strong sheath limit, i.e. $E_{\parallel} \rightarrow 0$ as $\Lambda \rightarrow \infty$.

Another way to describe the screening of E_{\parallel} is to compute the ratio of the voltage drops across the plasma and sheath regions. The voltage drop across the plasma is

$$V_{\text{pl}} \equiv \oint_{\text{plasma}} ds E_{\parallel} \approx - \int_{z=-L}^L dz E_{\parallel} , \quad (35)$$

where we use the whole interval ($-L < z < L$) to allow for cancellation in the dipole phasing case. Using Eq. (33), we find that the voltage drop across the plasma is given by

$$\frac{V_{\text{pl}}}{V_{\text{vac}}(0)} = \frac{-(\Delta/L) n_{zf}^2}{2\alpha \Lambda} \left(\frac{\sin(\eta_0 - \delta) + \sin(\eta_0 + \delta)}{\sin(\eta_0 - \delta) + (\Delta/L)(n_{zf}^2 - 1)\eta_0 \cos(\eta_0 - \delta)} \right) \quad (36)$$

The voltage drop V_{sh} across the sheath is given by Eqs. (21) and (23), and in monopole phasing we multiply V_{sh} by a factor of 2 to include the additive voltages from the sheaths at both ends. It does not make sense to calculate the voltage split for dipole phasing because both V_{sh} and V_{pl} vanish by symmetry.

Thus, in the remainder of this section we restrict the discussion to monopole phasing ($\delta = 0$). For this phasing, it can be shown that the ratio of plasma to sheath voltage (“voltage split”) is given by

$$\left| \frac{V_{\text{pl}}}{V_{\text{sh}} \Big|_{\text{M}}} \right| = \frac{\tan \eta_0}{\Lambda \eta_{0s}} \rightarrow \frac{1}{\Lambda} . \quad (37)$$

where the form after the arrow is obtained in the limit $\eta_0 \rightarrow 0$. (Recall that $n_{zf} \gg 1$ implies $\eta_0 \ll 1$ so the arrow denotes the high- k_{\parallel} limit.) Using Ohm’s Law with constant current in the sheath-plasma circuit, the monopole result for the voltage split is consistent

with the physical interpretation of Λ as the ratio of sheath impedance to plasma impedance.

In monopole phasing the effect of the jump in dielectric constant at the sheath-plasma interface is to concentrate the E_{\parallel} field in the sheath and to screen it from the plasma, as was seen by direct calculation in the previous section. In the limit $\Lambda \rightarrow \infty$ (large sheath capacitance) all of the voltage appears across the sheath in monopole phasing.

III. Self-consistent sheath: Child-Langmuir Law

In the previous sections, we have obtained solutions for E_{SW} and V_{sh} as functions of Δ . However, sheath theory imposes the following well-known nonlinear constraint, called the Child-Langmuir (CL) Law^{20,21}

$$\Delta = \lambda_D \left(\frac{eV_0}{T_e} \right)^{3/4}, \quad (38)$$

where $\lambda_D = (T_e / 4\pi n e^2)^{1/2}$ is the Debye length, $V_0 = 3T_e + C_{sh} V_{sh}$ is the “rectified” (dc) sheath potential including the Bohm contribution $V_{Bohm} \approx 3T_e$, and C_{sh} is an order unity rectification coefficient.⁶ For the present discussion, we assume $3T_e \ll V_{sh}$ (generally true for antenna sheaths) and take $V_0 \sim V_{sh}$. The CL condition must be satisfied to have a self-consistent solution for the sheath width Δ and voltage V_{sh} . In this section, we discuss the procedure for obtaining a self-consistent sheath solution.

We consider the general case and write Eq. (21) in the form

$$\hat{V} \equiv \frac{V_{sh}}{V_{vac}} = \frac{A(\Delta/L)}{B(\Delta/L) + C} \quad (39)$$

where the phase information for $V_{vac}(0)$ has been dropped and it is understood that V_{vac} is always evaluated in monopole phasing in this paper. The coefficients in Eq. (39) are defined as

$$A = n_{zf}^2 \eta_0 \cos(\eta_0 - \delta) \quad (40)$$

$$B = (n_{zf}^2 - 1)\alpha \eta_0 \cos(\eta_0 - \delta) \quad (41)$$

$$C = \alpha \sin(\eta_0 - \delta) \quad (42)$$

Solving for Δ/L in Eq. (39), we obtain

$$\frac{\Delta}{L} = \frac{C \hat{V}}{A - B \hat{V}} \quad , \quad (43)$$

and equating the resulting expression to Δ/L obtained from the Child-Langmuir Law, Eq. (38), one obtains a self-consistency constraint of the form

$$\frac{C \hat{V}^{1/4}}{A - B \hat{V}} = \left(\frac{\lambda_D}{L} \right) \left(\frac{eV_{vac}}{T_e} \right)^{3/4} \quad . \quad (44)$$

This nonlinear equation gives the self-consistent sheath voltage \hat{V} as a function of the phasing, the spectrum, and the vacuum-field sheath drive V_{vac} (which is a function of the rf antenna voltage or rf power). Recall from Eq. (26) that $\hat{V} \leq 1$ and the maximum value is obtained in the limit $(\Delta/L)n_{zf}^2 \rightarrow \infty$.

In Fig. 1, the self-consistent value of $\hat{V} \equiv V_{sh}/V_{vac}$ is plotted as a function of eV_{vac}/T_e for monopole phasing ($\delta = 0$, $\alpha = 1$) with the parameters $n_e = 10^{10} \text{ cm}^{-3}$, $T_e = 50 \text{ eV}$, and $n_{zf} = 10$. For these parameters, the factor $(\Delta/L)n_{zf}^2$ varies from 0 to 60 as eV_{vac}/T_e varies from 0 to 100. Note the nonlinear increase in \hat{V} for $eV_{vac}/T_e \gg 1$ (characteristic of Child-Langmuir Law scaling)⁹ and that $\hat{V} = V_{sh}/V_{vac} < 1$ for the range of parameters shown. For this case, the vacuum sheath model overestimates the self-consistent sheath voltage by less than a factor of two when $eV_{vac}/T_e > 40$.

IV. Summary and Conclusions

In this paper, we describe an analytic calculation of rf sheath voltages generated by electromagnetic waves propagating down a waveguide filled by a constant-density, tenuous plasma (i.e. $\epsilon_x = 0$ and $\epsilon_{\perp} = 1$ but $\epsilon_{\parallel} \gg 1$). The “waveguide” is meant as a simplified model of wave launching by an ICRF antenna, e.g. in the region in front of the Faraday screen and surrounded by the antenna protection limiters. In this region the fast wave propagates through a low density plasma, and the parasitically generated slow wave creates sheaths on the surrounding surfaces.

We assume that the fast wave is polarized in the y direction, propagates in the x direction, and satisfies boundary conditions at conducting walls located at $z = \pm L$. The magnetic field lines are oriented primarily in the z direction, but a small component of \mathbf{B} in the direction of the FW electric field is assumed, i.e. $b_y \equiv B_y / B \ll 1$. The wave propagation equations are solved by an expansion in the small parameter b_y with $k_y = 0$. One of the novel and important aspects of the calculation is the use of an rf sheath BC^{8,9} at the plasma-sheath interface. We have shown that the magnetic field tilt ($b_y \neq 0$) couples the FW to the SW, and this coupling is modified by the sheath capacitance (through the sheath BC) when $\Delta \neq 0$. In the self-consistent picture, the SW generates sheaths by accelerating electrons along \mathbf{B} , and the presence of the capacitive sheath adjacent to a plasma with large ϵ_{\parallel} modifies the SW fields, screening them from the plasma and enhancing them in the sheath region. It was demonstrated how to obtain a self-consistent solution for the rf fields at the sheath, the sheath width, and the sheath voltage by imposing the Child-Langmuir constraint.

The main quantitative results of this paper are the expressions for the SW rf electric field in Eq. (17), the rf sheath voltage in Eq. (21) and its monopole $n_z \gg 1$ limit in Eq. (25), the plasma E_{\parallel} in Eq. (33), and the nonlinear equation (44) derived using the Child-Langmuir constraint. This calculation illustrates some of the conceptual points

concerning rf wave propagation and sheath generation in the vicinity of a FW antenna, which were first studied with the vacuum-field sheath model.^{7,10} These include the role of magnetic field line tilt discussed above, and the phasing dependence of the sheath voltage for two-strap antennas (much larger in monopole than in dipole phasing because of the symmetry of the FW field). However, the main usefulness of the present calculation is to illustrate the modification of the sheath effects in the presence of plasma. For example, it was shown that the sheath voltage in the presence of plasma ($\epsilon_{\parallel} \gg 1$) is smaller than the vacuum field sheath voltage estimate $V = \oint ds E_{\parallel}$ for finite $(\Delta/L)n_{zf}^2$ [see Eq. (21) and Fig. 1]. Our calculation also demonstrates how the rf field distribution is modified by the presence of the sheath: the rf field E_{\parallel} is screened in the plasma region ($\propto 1/\epsilon_{\parallel}$) and increased in the sheath region; the corresponding ratio of voltages across the plasma (V_{pl}) and sheath (V_{sh}) scales as $|V_{pl}/V_{sh}| = 1/\Lambda$, where $\Lambda \equiv -\epsilon_{\parallel}(\Delta/L)$ measures the ratio of sheath capacitance to plasma inductance. The importance of the parameter Λ was also noted in the electrostatic SW model of Ref. 9.

The model for the rf sheath driving voltage V_{sh} described here can be used to calculate the rectified sheath potential $V_0 = 3T_e + C_{sh} V_{sh}$ (see Sec. III) and the “sheath power dissipation” $P_{sh} \propto n_i c_s (eV_0)$ due to ions accelerated out of the plasma by the sheaths (e.g. see Ref. 22 for a detailed discussion of P_{sh}). Here, the order unity rectification coefficient has the value $C_{sh} = 0.6$ for 0-to-peak values of the voltage.⁶

Apart from its pedagogical value, the most important application of this model is to guide the implementation of the sheath BC in antenna codes. (For example, this implementation is in progress for the TOPICA antenna code.²³) The analytic results derived here can be used for validation and verification (V&V) studies of antenna codes. Also, Eq. (21) could be used to obtain a better estimate of the rf sheath potential for experimental applications: one would compute $V_{vac} = -\int ds E_{\parallel}^{(vac)}$ using one of the

existing 3D antenna codes and then apply Eq. (21) to incorporate the effects of plasma ($\epsilon_{\parallel} \neq 0$) and of the sheath BC.

An interesting question is whether present experiments are in the regime where the vacuum sheath model is valid ($\hat{V} = V_{\text{sh}}/V_{\text{vac}} \sim 1$). Figure 1 suggests that the vacuum model is a reasonable approximation for sufficiently large voltages. In high power ICRF applications, the antennas typically couple several MW of power to the plasma and have voltage differences of tens of kV along the current straps. For typical field line mappings near the antenna, this can result in kV rf sheaths. For example, a previous modeling study of the TFTR Bay-M antenna¹⁰ yielded the following scaling²⁴ of the sheath voltage: $V_{\text{vac}}(\text{kV}) = 0.3 - 2.8 [P_{\text{rf}}(\text{MW})]^{1/2}$, where the range covers different phasings (monopole and dipole) and different types of field line connections (screen-screen, screen-limiter, etc.) Thus, typical antennas have sheaths which satisfy $eV_{\text{vac}}/T_e \gg 1$. The requirement for validity of the vacuum field model ($\hat{V} \sim 1$) is met when $(\Delta/L)n_{\text{zf}}^2 \gg 1$ is large [see Eq. (21)], which also depends on other parameters as well, notably the plasma density in the antenna region (determining ϵ_{\parallel} and Δ) and the antenna dimension L . Using $n_{\text{zf}} = k_{\text{zf}}c/\omega$ and $k_{\text{zf}}L = \pi/2$ (from the FW BC), and assuming monopole phasing, one sees that $\hat{V} \propto (\Delta/L)n_{\text{zf}}^2 \propto 1/L^3$; thus, \hat{V} decreases with L , the length of the field line connection between sheaths in the toroidal direction. In fact, numerical calculations of the self-consistent sheath voltage for typical parameters show that the decrease of \hat{V} with L is quite rapid. This effect is outside the scope of the vacuum field sheath model, but is addressed by the present calculation.

The present work uses the tenuous plasma approximation, valid when $\omega_{\text{pi}}^2/\omega^2 \ll 1$, which is appropriate near the Faraday screen where the density is low. In a future paper, we will discuss the additional plasma corrections when $\omega_{\text{pi}}^2/\omega^2 \geq 1$ required in the high density region farther into the plasma.

Acknowledgements

We thank the RF SciDAC team and the TOPICA group at the University of Torino for stimulating discussions. This work was supported by the U.S. Department of Energy (DOE) under DOE Grant Nos. DE-FG03-97ER54392 and DE-FC02-05ER54823; however, this support does not constitute an endorsement by the DOE of the views expressed herein.

References

- ¹ J.-M. Noterdaeme and G. Van Oost, *Plasma Phys. Control. Fusion* **35**, 1481 (1993).
- ² J. R. Myra, D. A. D'Ippolito, D. A. Russell, L. A. Berry, E. F. Jaeger, and M. D. Carter, *Nucl. Fusion* **46**, S455-S468 (2006).
- ³ F. W. Perkins, *Nucl. Fusion* **29**, 583 (1989).
- ⁴ R. Chodura and J. Neuhauser, in *Proceedings of the 16th European Conference on Controlled Fusion and Plasma Heating*, Venice (European Physical Society, Petit-Lancy, 1989) Vol. **13B**, Part III, p. 1089; R. Chodura, *Fusion Eng. Design* **12**, 111 (1990).
- ⁵ R. Van Niewenhove and G. Van Oost, *J. Nucl. Mat.* **162-164**, 288 (1989).
- ⁶ J. R. Myra, D. A. D'Ippolito, and M. J. Gerver, *Nucl. Fusion* **30**, 845 (1990).
- ⁷ D. A. D'Ippolito, J. R. Myra, M. Bures, and J. Jacquinot, *Plasma Phys. Controlled Fusion* **33**, 607 (1991).
- ⁸ J. R. Myra, D. A. D'Ippolito, and M. Bures, *Phys. Plasmas* **1**, 2890 (1994).
- ⁹ D. A. D'Ippolito and J. R. Myra, *Phys. Plasmas* **13**, 102508 (2006).
- ¹⁰ J. R. Myra, D. A. D'Ippolito, and Y. L. Ho, *Fusion Eng. Design* **31**, 291 (1996).
- ¹¹ L. Colas, S. Heuraux, S. Brémond and G. Bosia, *Nucl. Fusion* **45**, 767 (2005).
- ¹² R. Maggiora, private communication (2007).
- ¹³ F. Jaeger, L. A. Berry, J. S. Tolliver, and D. B. Batchelor, *Phys. Plasmas* **2**, 2597 (1995).
- ¹⁴ M. D. Carter, V. Godyak, D. Hoffman, W.S. Lee, D. Buchberger, and P. M. Ryan, *J. Appl. Phys.* **100**, 073305 (2006).
- ¹⁵ For an early discussion of the unmagnetized case, see G. Bekefi, *Radiation Processes in Plasmas* (Wiley, New York, 1966), pp. 168 – 173.

- ¹⁶ R. L. Stenzel, Phys. Rev. Lett. **60**, 704 (1988); Phys. Fluids B **1**, 2273 (1989) (and references therein).
- ¹⁷ J. R. Myra, D. A. D’Ippolito, D. W. Forslund and J. U. Brackbill, Phys. Rev. Lett. **66**, 1173 (1991).
- ¹⁸ M. A. Lieberman, A. J. Lichtenberg, E. Kawamura, Thomas Mussenbrock, and Ralf Peter Brinkmann, Phys. Plasmas **15**, 063505 (2008) (and references therein).
- ¹⁹ D. A. D’Ippolito, J. R. Myra, E. F. Jaeger, and L. A. Berry, Lodestar Report #LRC-07-113, submitted to Phys. Plasmas (2008).
- ²⁰ C. D. Child, Phys. Rev. **32**, 492 (1911); I. Langmuir, Phys. Rev. **21**, 419 (1923).
- ²¹ F. F. Chen, *Introduction to Plasma Physics* (Plenum Press, New York, 1974).
- ²² D. A. D’Ippolito and J. R. Myra, Phys. Plasmas **3**, 420 (1996).
- ²³ B. Van Compernelle, R. Maggiora, G. Vecchi, D. Milanesio and R. Koch, *35th EPS Conference on Plasma Phys., Hersonissos, 9 - 13 June 2008 ECA Vol.32, P-2.105 (2008)*
- ²⁴ see Table I and Eq. (3) in D. A. D’Ippolito, J. R. Myra, J. H. Rogers, K. W. Hill, J. C. Hosea, R. Majeski, G. Schilling, J. R. Wilson, G. R. Hanson, A. C. England, and J. B. Wilgen, Nucl. Fusion **38**, 1543 (1998).

Figure Captions

Fig. 1 Plot of the self-consistent (Child-Langmuir) sheath voltage, V_{sh}/V_{vac} , vs the “vacuum field” sheath drive, eV_{vac}/T_e , obtained from the solution of Eq. (39). This plot assumes monopole phasing with the parameters $n_e = 10^{10} \text{ cm}^{-3}$, $T_e = 50 \text{ eV}$, and $n_{zf} = 10$.

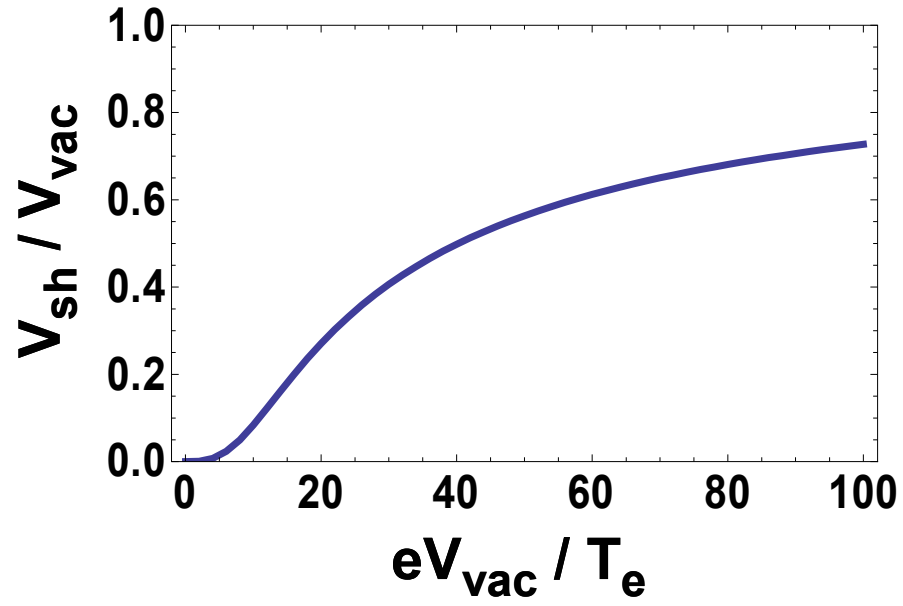


Fig. 1 Plot of the self-consistent (Child-Langmuir) sheath voltage, $V_{\text{sh}} / V_{\text{vac}}$, vs the “vacuum field” sheath drive, eV_{vac} / T_e , obtained from the solution of Eq. (39). This plot assumes monopole phasing with the parameters $n_e = 10^{10} \text{ cm}^{-3}$, $T_e = 50 \text{ eV}$, and $n_{zf} = 10$.